DRAFT

(2)

AN ANALYSIS OF POOL SURFACE DEFORMATION DUE TO A PLUNGING LIQUID JET

F. Bonetto
D.A. Drew
R.T. Lahey, Jr.
Center for Multiphase Research
Rensselaer Polytechnic Institute
Troy, NY 12180-3590 USA

N00014-91-J-1271
JUNE 1992

ABSTRACT

When a liquid jet impacts a pool containing the same liquid and surrounded by a still gas, a surface depression is produced. The surface shape is determined by the Weber number, $We = \frac{\frac{1}{2}\rho_\ell v_\ell^2 x_o}{\sigma}$. In this work the shape of the surface is obtained as a function of the Weber number by using an asymptotic expansion technique.

INTRODUCTION

The entrainment of non-condensible gases by a plunging liquid jet impacting a liquid pool is related to some important practical problems. For example, the absorption of greenhouse gases into the ocean has been hypothesized to be highly dependent upon the air carryunder that occurs during breaking waves, which represent a type of plunging jet [Monahan, 1991; Kerman, 1984]. Other applications include some type of liquid/gas chemical reactors. In order to enhance the reaction rate, a jet of liquid entrains the surrounding gas reactant forming a two-phase jet. The reaction rate is enhanced because of the increase of the interfacial area density and the pseudo-turbulence produced by the entrained gas bubbles.

Other less obvious applications are associated with the slug or plug flow regimes. For example, in vertical slug flow, the Taylor bubbles move upward with an almost constant velocity. The liquid film surrounding the Taylor bubbles

drains downward forming an annular liquid jet. Therefore, a gas entrainment problem, similar to the one studied in this work, occurs behind the Taylor bubbles. In particular, a Helmholtz-Kelvin instability occurs at the interface in the rear portion of the Taylor bubble such that smaller gas bubbles are entrapped in the liquid plug behind the Taylor bubble. A difference with respect to this work is that in the slug flow case the velocity distribution is nonuniform while in this work a uniform velocity distribution was assumed.

DISCUSSION

Most prior theoretical studies were done for liquid jets with very low liquid velocity, which had applications for the coating of fiber, etc. Recently, Lezzi & Prosperetti [1991] performed a stability analysis considering the liquid jet and the pool to be inviscid liquids and the gas to be viscous. They did not analyze the surface depression.

Bonetto, et al [1992] analyzed an inclined plunging liquid jet. They assumed that both the gas and the liquid were inviscid and they obtained the entrained gas flow rate. The entrained gas volumetric flow rate is one of the most important quantities which we want to compute in problems of this type. The key parameter in such evaluations is a knowledge of the gas gap thickness (ie, the shape of the inclined surface depression.

The objective of this work was to evaluate the induced surface depression caused by an impacting liquid jet. We have assumed that both fluids are inviscid and irrotational, and that the gas region is at constant pressure. Hence the appropriate equation for this problem is the Laplace equation for the liquid and the associated interfacial jump condition. The former equation has no parameter

and the latter has only the Weber number, $We = \frac{\frac{1}{2}\rho_\ell v_\ell^2 x_o}{\sigma}$, where x_o is the half-width of the liquid jet.

We may use an asymptotic expansion technique to solve the problem. That is, we may expand the solutions in terms of relatively small We number, and substitute these expressions into the Laplace equation and the interfacial jump condition.

Equating terms of the same order in We, one obtains a recursive system of equations, which can be numerically evaluated up to third order. In other words, we can evaluate the eigenfunctions of the problem. Once we have these eigenfunctions we can compute the shape of the surface (and the velocity fields) as a function of the We numbers.

ASYMPTOTIC EXPANSION

The purpose of this section is to compute the position of the interface, $\eta(x)$ (shown schematically in Figure-1).

For the assumption of irrotational, inviscid flow the governing equations for the liquid field are

$$\nabla^2 \hat{\psi} = 0 \tag{1}$$

where $\hat{\psi}$ is the stream function. The two velocity components are evaluated as,

$$\hat{u} = \frac{\partial \hat{\psi}}{\partial \hat{y}} \tag{2}$$

$$\hat{v} = -\frac{\partial \hat{\psi}}{\partial \hat{x}} \tag{3}$$

where $\hat{u}$ and $\hat{v}$ are the velocity components along the $\hat{x}$ and $\hat{y}$ axis, respectively. If we prescribe a value of $\hat{\psi}$, or its derivatives normal to the surface, $\frac{\partial \hat{\psi}}{\partial \hat{u}}$, for every point on the boundary we have a well posed problem. As shown in Fig.-2, the plane $\hat{x} = 0$ is a symmetry plane then the lateral u velocity must vanish for every $\hat{y}$ at $\hat{x} = 0$. Using Eq. (2)

$$\hat{u}(\hat{x} = 0, \hat{y}) = \frac{\partial \hat{\psi}}{\partial \hat{y}} (\hat{x} = 0, \hat{y}) = 0 \tag{4}$$

on the centerline of the plunging liquid jet. We know that the v-velocity must be $\hat{v}_\ell$ at positions where the jet is impacting. From Figure-1 and Eq. (3), we see that:

$$\hat{v}\ (0 < \hat{x} < x_0, \hat{y} = 0) = -\frac{\partial \hat{\psi}}{\partial \hat{x}} (0 < \hat{x} < x_0, \hat{y} = 0) = \hat{v}_\ell \tag{5}$$

For $\hat{x} > x_0$, the free surface position, $\hat{\eta}(\hat{x})$, must be coincident with a streamline. Without loosening generality we make the free surface coincident with the streamline $\hat{\psi} = 0$, then

$$\hat{\psi}\left(\hat{x}, \hat{\eta}(\hat{x})\right) = 0 \tag{6}$$

We may assume that the pressure in the gas region is constant and equal to zero. The liquid pressure right under the surface is related to the curvature of the surface by:

$$\frac{\sigma \dfrac{d^2\hat{\eta}}{d\hat{x}^2}}{\left(1 + \left(\dfrac{d\hat{\eta}}{d\hat{x}}\right)^2\right)^{3/2}} = \hat{P}_\ell (\hat{x}, \hat{\eta}(\hat{x})) = -\frac{1}{2} \rho_\ell \left[\hat{u}^2(\hat{x}, \hat{\eta}(\hat{x})) + \hat{v}^2(\hat{x}, \hat{\eta}(\hat{x}))\right] \tag{7}$$

where, σ, P_ℓ, ρ_ℓ, η are the surface tension, liquid pressure, liquid density and position of the interface, respectively, and $\hat{u}^2(\hat{x},\hat{\eta}(\hat{x}))$ and $\hat{v}^2(\hat{x},\hat{\eta}(\hat{x}))$ are the u and v velocity components.

In order to have a well-posed problem we may specify $\hat{\psi}$ for $\hat{x} \to \infty$ for every $\hat{y}$, $\hat{\psi}$ $(\hat{x} \to \infty,\hat{y})$ and $\hat{\psi}$ $(\hat{x},\hat{y} \to \infty)$. One possible set of boundary conditions is:

$$\hat{\psi}\ (\hat{x} \to \infty,\hat{y}) = 0 \tag{8}$$

$$\hat{\psi}\ (\hat{x},\hat{y} \to \infty) = 0 \tag{9}$$

We make Eqs. (1)-(9) nondimensional, using x_0, v_ℓ as the length scale and velocity scale, respectively. It is convenient to work with nondimensional quantities. Thus we have:

$$\nabla^2\psi = 0 \tag{10}$$

with boundary conditions,

$$\frac{\partial\psi}{\partial y}(x = 0, y) = 0 \tag{11a}$$

$$\psi\,(x, y\to\infty) = 0 \tag{11b}$$

$$\psi\,(x\to\infty,y) = 0 \tag{11c}$$

$$\frac{\partial\psi}{\partial x}(x, y=0) = -\,1 \qquad 0 < x < 1 \tag{11d}$$

$$\psi(x,\eta\,(x)) = 0 \qquad 1 < x \tag{11e}$$

where,

$$u = \hat{x}/x_0 \quad , \quad y = \hat{y}/x_0 \quad , \quad \eta = \hat{\eta}/x_0$$

$$x = \hat{u}/V_\ell \quad , \quad v = \hat{v}/V_\ell \quad \text{and} \quad \psi = \frac{\hat{\psi}}{x_0 V_\ell}$$

The velocity components may be computed from the stream function using Eqs. (2) and (3) as,

$$u(x,y) = \frac{\partial \psi}{\partial y}(x,y) \tag{12}$$

$$v(x,y) = \frac{\partial \psi}{\partial x}(x,y) \tag{13}$$

The system of equations is closed with

$$\frac{d^2\eta/dx^2}{\left(1 + (\frac{d\eta}{dx})^2\right)^{3/2}} = \left(\frac{1}{2}\rho_\ell \frac{V_\ell^2 x_0}{\sigma}\right)\left[u^2(x,\eta(x)) + v^2(x,\eta(x))\right] \tag{14}$$

Notice that the only parameter is the Weber number, $We = \frac{1}{2}\rho_\ell \frac{V_\ell^2 x_0}{\sigma}$, which appears in the boundary condition, Eq. (14),

In rder to solve the problem analytically we would have to get a solution of the Laplace equation, Eq. (10) that satisfies the boundary conditions, eq. (11), where the free surface depression, $\eta(x)$, comes from Eq. (14). Notice that the solution of Eq. (14) is linked to the solution of ψ through u and v, thus the problem is highly nonlinear.

Fortunately we use an asymptotic expansion technique. First, we may expand all the dependent variables in terms of the We number obtaining:

$$\eta(x) = \sum_{i=0}^{n} We^i \eta_i(x) + O(We^{n+1}) \tag{15a}$$

$$\psi(x,y) = \sum_{i=0}^{n} We^i \psi_i(x,y) + O(We^{n+1}) \tag{15b}$$

$$u(x,y) = \sum_{i=0}^{n} We^i u_i(x,y) + O(We^{n+1}) \tag{15c}$$

$$v(x,y) = \sum_{i=0}^{n} We^i v_i(x) + O(We^{n+1}) \tag{15d}$$

Next we substitute Eq. (15b) into Eq. (10) to obtain,

$$\nabla^2\psi = \nabla^2\psi_0 + We\nabla^2\psi_1 + We^2\nabla^2\psi_2 + \ldots = 0 \tag{16}$$

Equation (16) holds for all We, and thus all ψ_i must independently satisfy Laplace equations:

$$\nabla^2\psi_0 = 0 \tag{17a}$$

$$\nabla^2\psi_1 = 0 \tag{17b}$$

$$\nabla^2\psi_2 = 0 \tag{17c}$$

Using the same reasoning, it is easy to show that all the homogeneous boundary conditions, Eqs. (11a) - (11c) lead to:

$$\frac{\partial\psi_i}{\partial y}(x=0,y) = 0 \qquad i \geq 0 \tag{18}$$

$$\psi_i(x,y\to\infty) = 0 \qquad i \geq 0 \tag{19}$$

$$\psi_i(x\to\infty,y) = 0 \qquad i \geq 0 \tag{20}$$

Let us next expand the boundary condition in Eq. (11d):

$$\frac{\partial \psi_o}{\partial x}(x,y=0) + We\frac{\partial \psi_1}{\partial x}(x,y=0) + We^2\frac{\partial \psi_2}{\partial x}(x,y=0) + \ldots = -1 \qquad (21)$$

Obviously the zeroth order term must be equal to -1 and all other terms must be zero. Thus,

$$\frac{\partial \psi_o}{\partial x}(x,y=0) = -1 \qquad (22)$$

and

$$\frac{\partial \psi_i}{\partial x}(x,y=0) = 0 \qquad i \geq 1 \qquad (23)$$

The boundary condition in Eq. (11e), and the interfacial jump contidion, Eq. (14), require special attention. Using Eq. (15b), Eq. (11e) can be rewritten as:

$$0 = \psi(x,\eta(x)) = \psi_o(x,\eta(x)) + We\,\psi_1(x,\eta(x)) + We^2\psi_2(x,\eta(x)) + \ldots \qquad (24)$$

Performing an expansion in terms of We in the neighborhood of $\eta = 0$, we obtain:

$$0 = \psi_o(x,0) + \frac{\partial \psi_o}{\partial y}(x,0)\eta(x) + \frac{1}{2}\frac{\partial^2 \psi_o}{\partial y^2}(x,0)\eta^2(x) + \ldots$$

$$+ We\left[\psi_1(x,0) + \frac{\partial \psi_1}{\partial y}(x,0)\,\eta(x) + \frac{1}{2}\frac{\partial^2 \psi_1}{\partial y^2}(x,0)\eta^2(x) + \ldots\right] + \ldots \qquad (25)$$

Substituting Eqs. (15a) and (12) into Eq.(25), and rearranging (ie, collecting terms We^i), we obtain:

$$0 = \psi_o(x,0) + \left[u_o(x,0)\,\eta_1(x) + \psi_1(x,0)\right]We$$

$$+ We^2\left(u_1\eta_1 + u_o\eta_2 + \frac{1}{2}\frac{\partial u_o}{\partial y}\eta_1^2 + \psi_2(x,0)\right)$$

$$+ We^3\left(u_1\eta_2 + \frac{1}{2}\frac{\partial u_1}{\partial y}\eta_1^2 + u_2\eta_1 + u_o\eta_3 + \frac{\partial u_o}{\partial y}\eta_1\eta_2 + \frac{1}{6}\eta_1^3 + \psi_3(x,0)\right) + We^4 \quad ...(26)$$

Thus, the boundary conditions for $x > 1$ are

$$\psi_o(x,0) = 0 \tag{27a}$$

$$\psi_1(x,0) = - u_o\eta_1 \tag{27b}$$

$$\psi_2(x,0) = -\left(u_1\eta_1 + u_o\eta_2 + \frac{1}{2}\frac{\partial u_o}{\partial y}\eta_1^2\right) \tag{27c}$$

$$\psi_3(x,0) = -\left(u_o\eta_3 + u_1\eta_2 + u_2\eta_1 + \frac{1}{2}\frac{\partial u_1}{\partial y}\eta_1^2 + \frac{\partial u_o}{\partial y}\eta_1\eta_2 + \frac{1}{6}\frac{\partial^2 u_o}{\partial y}\eta_1^3\right) \tag{27d}$$

Notice that ψ_i has homogeneous boundary conditions for $i \geq 1$ except for $x \geq 1$ where its value is given by Eqs. (27). This set of equations is the result of the asymptotic expansion of Eq. (11e). In order to get a closed set of equations, let us focus our attention on Eq. (14), the interfacial jump condition. We first expand the left hand side of Eq. (14) and then the right hand side.

The left hand side of Eq. (14) can be rewritten as:

$$\frac{d^2\eta/dx^2}{\left(1 + (\frac{d\eta}{dx})^2\right)^{3/2}} = \frac{\frac{d^2}{dx^2}\left(\sum_{i=0}^{n} \eta_i(x)\, We^i + O(We^{n+1})\right)}{\left\{1 + \left[\frac{d}{dx}\left(\sum_{i=0}^{n} \eta_i(x)\, We^i + O(We^{n+1})\right)\right]^2\right\}^{3/2}}$$

$$= \frac{d^2\eta_o}{dx^2} + \frac{d^2\eta_1}{dx^2}We + \frac{d^2\eta_2}{dx^2}We^2 + We^3\left(-\frac{3}{2}\frac{d^2\eta_1}{dx^2}\left(\frac{d\eta_1}{dx}\right)^2 + \frac{d^2\eta_3}{dx^2}\right)$$

$$+ We^4\left(-3\frac{d^2\eta_1}{dx^2}\frac{d\eta_1}{dx}\frac{d\eta_2}{dx} - \frac{3}{2}\frac{d^2\eta_2}{dx^2}\left(\frac{d\eta_1}{dx}\right)^2 + \frac{d^2\eta_4}{dx^2}\right) + O(We^5) \tag{28}$$

Similarly, the right hand side of Eq. (14) can be rewritten as,

$$We\left[u^2(x,\eta(x)) + v^2(x,\eta(x))\right] =$$

$$We\left\{\left[u_o(x,0) + \frac{\partial u_o}{\partial y}(x,0)\,\eta(x) + \frac{1}{2}\frac{\partial^2 u_o}{\partial y^2}(x,0)\,\eta^2(x) + \ldots\right.\right.$$

$$\left. + We\left(u_1(x,0) + \frac{\partial u_i}{\partial y}(x,0)\,\eta(x) + \frac{1}{2}\frac{\partial^2 u_1}{\partial y^2}(x,0)\eta^2(x) + \ldots\right)\right]^2$$

$$+\left[v_o(x,0) + \frac{\partial v_o}{\partial y}(x,0)\,\eta(x) + \frac{1}{2}\frac{\partial v_o}{\partial x^2}(x,0)\,\eta^2(x) + \ldots\right.$$

$$\left.\left. + We\left(v_1(x,0) + \frac{\partial v_1}{\partial y}(x,0)\eta(x) + \frac{1}{2}\frac{\partial^2 v_1}{\partial y^2}(x,0)\,\eta^2(x) + \ldots\right)\right]^2\right\} \qquad (29)$$

Using Eq. (15a) we obtain:

$$We\left[u^2(x,\eta(x)) + v^2(x,\eta(x))\right]$$

$$= We\left\{\left[u_o(x,0) + \frac{\partial u_o}{\partial y}(x,0)\,(\eta_o + We\eta_1 + We^2\eta_2 + \ldots) + \ldots\right.\right.$$

$$\left. + We\left(u_1(x,0) + \frac{\partial u_1}{\partial y}(x,0)\,(\eta_o + We\eta_1 + We^2\eta_2 + \ldots)\right)\right]^2$$

$$+\left[v_o(x,0) + \frac{\partial v_o}{\partial y}(x,0)\left(\eta_o(x) + We\eta_1 + We^2\eta_2 + \ldots\right) + \ldots\right.$$

$$\left.\left. + We\left(v_1(x,0) + \frac{\partial v_1}{\partial y}(x,0)\left(\eta_o + We\eta_1 + We^2\eta_2 + \ldots\right) + \ldots\right) + \ldots\right]^2\right\} \qquad (29b)$$

Finally, we obtain

$$(u^2+v^2)\,We = (u_o^2+v_o^2)\,We + We^2\left(2u_o\left(\frac{\partial u_o}{\partial y}\eta_1+u_1\right)+2v_o\left(\frac{\partial v_o}{\partial y}v_1+v_1\right)\right)$$

$$+ We^3\left\{\left[\frac{\partial v_o}{\partial y}\eta_1+v_1\right]^2+2\,v_o\left[\frac{\partial v_1}{\partial y}\eta_1+\frac{\partial v_o}{\partial y}\eta_2+\frac{1}{2}\frac{\partial_2 v_o}{\partial y^2}\eta_1^2+v_2\right]+\left[\frac{\partial u_o}{\partial y}v_1+u_1\right]^2\right.$$

$$\left.+\,2u_o\left[\frac{\partial u_1}{\partial y}\eta_1+\frac{\partial u_o}{\partial y}\eta_2+\frac{1}{2}\frac{\partial^2 u_o}{\partial y^2}+u_2\right]\right\}$$

$$+ We^4\left\{2\left[\frac{\partial v_o}{\partial y}\eta_1+v_1\right]\left[\frac{\partial v_1}{\partial y}\eta_1+\frac{\partial v_o}{\partial y}\eta_2+\frac{1}{2}\frac{\partial^2 v_o}{\partial y^2}\eta_1^2+v^2\right]\right.$$

$$+\,2v_o\left[\frac{\partial v_1}{\partial y}\eta_2+\frac{1}{2}\frac{\partial^2 v_1}{\partial y^2}\eta_1^2+\frac{\partial v_2}{\partial y}\eta_1+\frac{\partial v_o}{\partial y}\eta_3+\frac{\partial^2 v_o}{\partial y^2}\eta_1\eta_2+\frac{1}{6}\frac{\partial^3 v_o}{\partial y}\eta_1^3+v_3\right]$$

$$+\,2u_o\left[\frac{\partial u_1}{\partial y}\eta_2+\frac{1}{2}\frac{\partial^2 u_1}{\partial y^2}\eta_1^2+\frac{\partial u_2}{\partial y}\eta_1+\frac{\partial u_o}{\partial y}\eta_3+\frac{\partial^2 u_o}{\partial y^2}\eta_1\eta_2+\frac{1}{6}\frac{\partial^3 u_0}{\partial y^3}\eta_1^3+u_3\right]$$

$$\left.+\,2\left[\frac{\partial u_o}{\partial y}\eta_1+u_1\right]\left[\frac{\partial u_1}{\partial y}\eta_1+\frac{\partial u_o}{\partial y}\eta_2+\frac{1}{2}\frac{\partial^2 u_o}{\partial y^2}\eta_1^2+u_2\right]\right\}+\ldots \qquad (30)$$

Comparing the expression for the left hand side of Eq. (28) with the right hand side of Eq. (30) we obtain:

$$\frac{d^2\eta_o}{dx^2}=0 \qquad (31a)$$

$$\frac{d^2\eta_1}{dx^2}=-\,(u_o^2+v_o^2) \qquad (31b)$$

$$\frac{d^2\eta_2}{dx^2}=-\left(2\,u_o\left(\frac{\partial u_o}{\partial y}\eta_1+u_1\right)+2\,v_o\left(\frac{\partial v_o}{\partial y}\eta_1+v_1\right)\right) \qquad (31c)$$

The boundary conditions for these ordinary differential equations are:

$$\eta_i\,(x\to\infty) = 0 \tag{32a}$$

$$\frac{d\eta_i}{dx}(x\to\infty) = 0 \tag{32b}$$

Equations (27) and (31) are the expanded forms of Eqs. (11e) and (14), respectively. Equations (17), (18), (19), (20), (22) and (23) complete the set of equations to be solved.

ORDER ZERO SOLUTION

In the previous section we establidshed a set of infinite coupled equations for $\eta_i(x)$. In this section we will analytically solve the order zero equation (i.e., the functions η_o, ψ_o, u_o, v_o). The equation for η_o is Eq. (31a),

$$\frac{d^2\eta_o}{dx^2} = 0$$

with the boundary conditions

$$\eta_o(x\to\infty) = 0 \tag{33a}$$

$$\frac{d\eta_o}{dx}(x\to\infty) = 0 \tag{33b}$$

The solution is

$$\eta_o(x) = 0 \tag{34}$$

The differential equation for ψ_o is Eq. (17a),

$$\nabla^2\psi_o = 0$$

and the corresponding boundary conditions, Eqs. (18), (19), (20), (22) and (23) are:

$$\psi_o(x\to\infty,y) = 0 \tag{35a}$$

$$\psi_o(x,y\to\infty) = 0 \tag{35b}$$

$$\frac{\partial\psi_o}{\partial y}(x=0,y) = 0 \tag{35c}$$

$$\frac{\partial\psi_o}{\partial x}(x,y=0) = -1 \qquad 0<x<1 \tag{35d}$$

$$\frac{\partial\psi_o}{\partial x}(x,y=0) = 0 \qquad x>1 \tag{35e}$$

It is convenient to use complex variables to solve the two-dimensional problem. Let Φ be a nondimensional analytic function given by,

$$\Phi(z) = \phi(x,y) + i\,\psi(x,y) \tag{36}$$

and

$$z = x + i\,y$$

and ϕ, ψ are the real and imaginary parts of $\Phi(z)$ respectively. The function $\Phi(z)$ is the complex potential, ϕ is the potential function and ψ is the steam function. The velocity components of u, v are given by

$$u = \frac{\partial\phi}{\partial x} = \frac{\partial\psi}{\partial z} \tag{37a}$$

$$u = \frac{\partial\phi}{\partial y} = -\frac{\partial\psi}{\partial x} \tag{37b}$$

and,

$$\frac{d\Phi}{dz} = u - i\,v \tag{38}$$

We recall the boundary conditions (35d&e),

$$\frac{\partial \psi_o}{\partial x}(x,0) = \begin{cases} -1 & 0 < x < 1 \\ 0 & x > 1 \end{cases} \tag{39}$$

A function of x and y that verifies these boundary conditions is:

$$\frac{\partial \psi_o}{\partial x} = \frac{1}{\pi}\left[\text{atg}\left(\frac{x-1}{y}\right) - \text{atg}\left(\frac{x+1}{y}\right)\right] \tag{40}$$

This expression is the imaginary part of the following analytic function

$$\frac{d\Phi}{dz} = \frac{1}{\pi}\left[\log(z-1) - \log(z+1)\right] \tag{41}$$

We may use Eq. (38) to calculate the velocity components

$$u_o = \text{Re}(\Phi)\left(\log\left[y^2 + (x-1)^2\right] - \log\left[y^2 + (x+1)^2\right]\right) \tag{42}$$

$$v_o = -\text{Im}(\Phi) = \frac{1}{\pi}\left(\text{atg}\frac{(x+1)}{y} - \text{atg}\frac{(x-1)}{y}\right) \tag{43}$$

Table-I shows the velocity of the zeroth order solution as well as the derivatives needed for solving Eqs. (27) and (31). We now have the solution of the problem to order zero. In order to solve the problem to order-n, we must:

(1) Compute $u_o(x,y=0)$ and $v_o(x,y=0)$ using Eqs. (42) and (43).

(2) Solve $\frac{d^2\eta_1}{dx^2}$ as a function of $u_o(x,0)$, $v_o(x,0)$ (Eq. (36)) with the the proper initial conditions (Eq. (32)).

(3) Compute $\psi_1(x,0)$ from Eq. (27b) for $x > 1$ using $\eta_1(x)$, $u_o(x,0)$, $v_o(x,0)$.

(4) Solve $\nabla^2\psi_1 = 0$ using $\psi_1(x,0)$.

(5) Compute $u_1(x,0) = \frac{\partial \psi_1}{\partial y}(x,0)$, $v_1(x,0)$, $= -\frac{\partial \psi_1}{\partial x}(x,0)$.

TABLE-I

SUMMARY OF THE ORDER-ZERO SOLUTIONS

$$u_o(x,0) = \frac{1}{\pi} \log \frac{x-1}{x+1}$$

$$v_o(x,0) = 0$$

$$\frac{\partial u_o}{\partial y}(x,0) = 0$$

$$\frac{\partial v_o}{\partial y}(x,0) = \frac{2}{\pi(x-1)(x+1)}$$

$$\frac{\partial^2 u_o}{\partial y^2}(x,0) = \frac{4x}{\pi(x-1)^2(x+1)^2}$$

$$\frac{\partial^2 v_o}{\partial y^2}(x,0) = 0$$

$$\frac{\partial^3 u_o}{\partial y^3}(x,0) = 0$$

$$\frac{\partial^3 v_o}{\partial y^3}(x,0) = -\frac{4(3x^2+1)}{\pi(x-1)^3(x+1)^3}$$

$$u_o(x,y) = \frac{1}{2\pi} \log \left(\frac{y^2 + (x-1)^2}{y^2 + (x+1)^2} \right)$$

$$v_o(x,y) = \frac{1}{\pi} \left(\text{atg} \frac{x+1}{y} - \text{atg} \frac{x-1}{y} \right)$$

(6) Evaluate $\frac{d^2\eta_2}{dx^2}$ using Eq. (31c).

(7) Compute $\psi_2(x,0)$ from Eq. (27c) for $x > 1$, using η_1, η_2, u_0, v_0', u_1, v_1.

(8) Solve $\nabla^2\psi_2 = 0$ using $\psi_2(x,0)$.

RESULTS

Figure-3 shows the analytical results for the solution of zeroth order transverse velocity, u_0^+ computed at $y = 0$.

We have shown that $\eta_0(x)$ is zero. The results for $\eta_1(x)$ are shown in Figure-4. This is the first correction term in the shape of the interface. Using $\eta_1(x)$ and $u_0(x,0)$ we can compute $\psi_1(x,0)$ from Eq. (27b), the non-homogeneous boundary condition for $\psi_1(x,y)$. Figure-5 shows the curves of constant ψ_1 obtained with PHOENICS [Spalding, 1991]. Now, we have the problem solved up to first order. We could compute the position of the surface in two possible different ways. First, from $\eta_1(x)$, and secondly from Eq. (15b)

$$\psi_0(x,y) + We\ \psi_1(x,y) = 0 \tag{44}$$

It is interesting to note that these do not produce the same result. The reason being that we did not solve the complete system of equations. In other words, if we compute the shape of the interface as,

$$\eta(x) = \sum_{i=0}^{\infty} We^i \eta_i(x) \tag{45}$$

where $\eta(x)$ will be equal to the $y(x)$ obtained from the equation

$$\sum_{i=0}^{\infty} We^i \psi_i(x,y) = 0 \qquad (46)$$

However, if we truncate the series and we compute only a finite number of terms, we will not get the same result for the surface from the two methods. From the result of $\psi_1(x,y)$ we can compute the velocity components $u_1(x,0)$, $v_1(x,0)$. Figure-6 shows $u_1(x,0)$ and $v_1(x,0)$.

Figures 7-8 show the contour maps for ψ_2 and ψ_3, respectively. Figure-9 shows the velocity components corresponding to the stream function ψ_2. Figures 10 and 11 show the second order eigenfunctions in η, i.e., η_2 and η_3. Figure-12 gives η x), the shape of the interface, for five different Weber numbers (ie, We = 0.1, 0.2, 0.3., 0.4 and 0.5). We arbitarily define the width of the gap between the interaces (δ) as the width corresponding to half the depth of the depression. Figure-13 defines the gas gap width (δ). Figure 14 depicts the width of the gas gap as a function of the Weber number obtained from Figure-12 using the definition from Figure-13.

SUMMARY AND CONCLUSIONS

This paper presents the results of an analysis based on asymptotic expansions for the surface depression produced by a plunging liquid jet. The first three terms of a Taylor series expansion in the Weber number have been obtained for the surface depression. This approximation of the surface depression gives correct values for small and moderate Weber numbers (ie, We < 1). However, for We greater than unity, higher order terms become important and the analysis presented here is no longer valid.

The results described in this paper show that as the Weber number is increased, the terms that gain importance (i.e., the terms of higher order)

correspond to a surface depression that is increasingly narrower in the horizontal direction. For a Weber number of the order of unity the surface tension is no longer strong enough to keep the system stable and an instability leads to air entrainment. That is, for values of the surface tension going to infinity (i.e., Weber number going to zero), the slope of the surface is very small, however, as the Weber number is increased the slope also increases. For a critical value of the Weber number, the slope of the surface is such that the surface tension is not large enough to keep the pool surface from touching the plunging liquid jet and thus air entrainment is produced.

The results presented in this paper cannot predict the route to instability that produces air entrainment for two reasons. First, it is not clear that the approximation of the surface depression is valid for Weber numbers that are high enough to produce air entrainment. Second, the shape of the surface, $\eta(x)$, has to be a monovalued function of x and it appears that at the point where air entrainment is produced, for every x (horizontal position) there is more than one η (vertical position of the surface depression).

It appears that it would be useful to compute the surface position using an appropriate multidimensional Computational Fluid Dynamics (CFD) tool having surface tracking capability. This will allow the relaxation of the small and moderate Weber numbers assumption.

ACKNOWLEDGMENT

The financial support given this study by the Office of Naval Research (ONR) is gratefully acknowledged.

REFERENCES

Bonetto, F., Drew, D.A. and Lahey, R.T., Jr., "The Analysis of a Plunging Jet - The Air Entrainment Process," submitted to *J. of Chemical Engineering Communications*, 1992.

Kerman, B.R., "A Model of Interfacial Gas Transfer for a Well-Roughened Sea," *J. of Geophysical Research*, Vol. 89 (D1), pp. 1439-1446, 1984.

Lezzi, A.M. and Prosperetti, A., "The Stability of an Air Film in a Liquid Flow," *J. Fluid Mech.*, Vol. 226, pp. 319-347, 1991.

Monahan, R. and Torgersen, T., in *Air-Water Mass Transfer*, ed. Wilhelms and Gulliver, pp. 608-617, 1991.

Spalding, B., "PHOENICS 1.6 - User's Manual," CHAM Ltd., 1991.

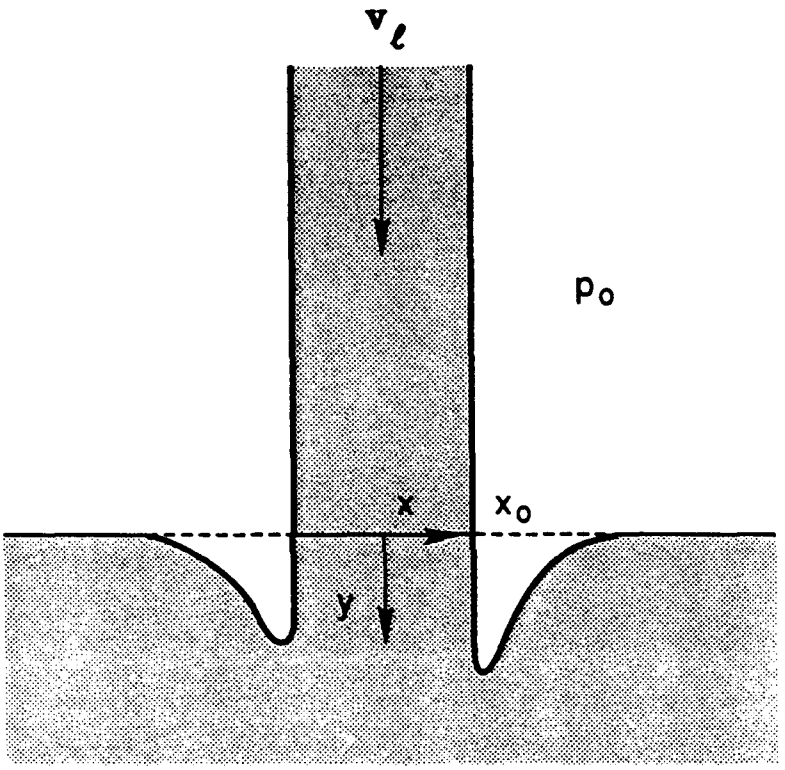

Figure 1 **Deformation of the pool surface produced by a plunging liquid jet.**

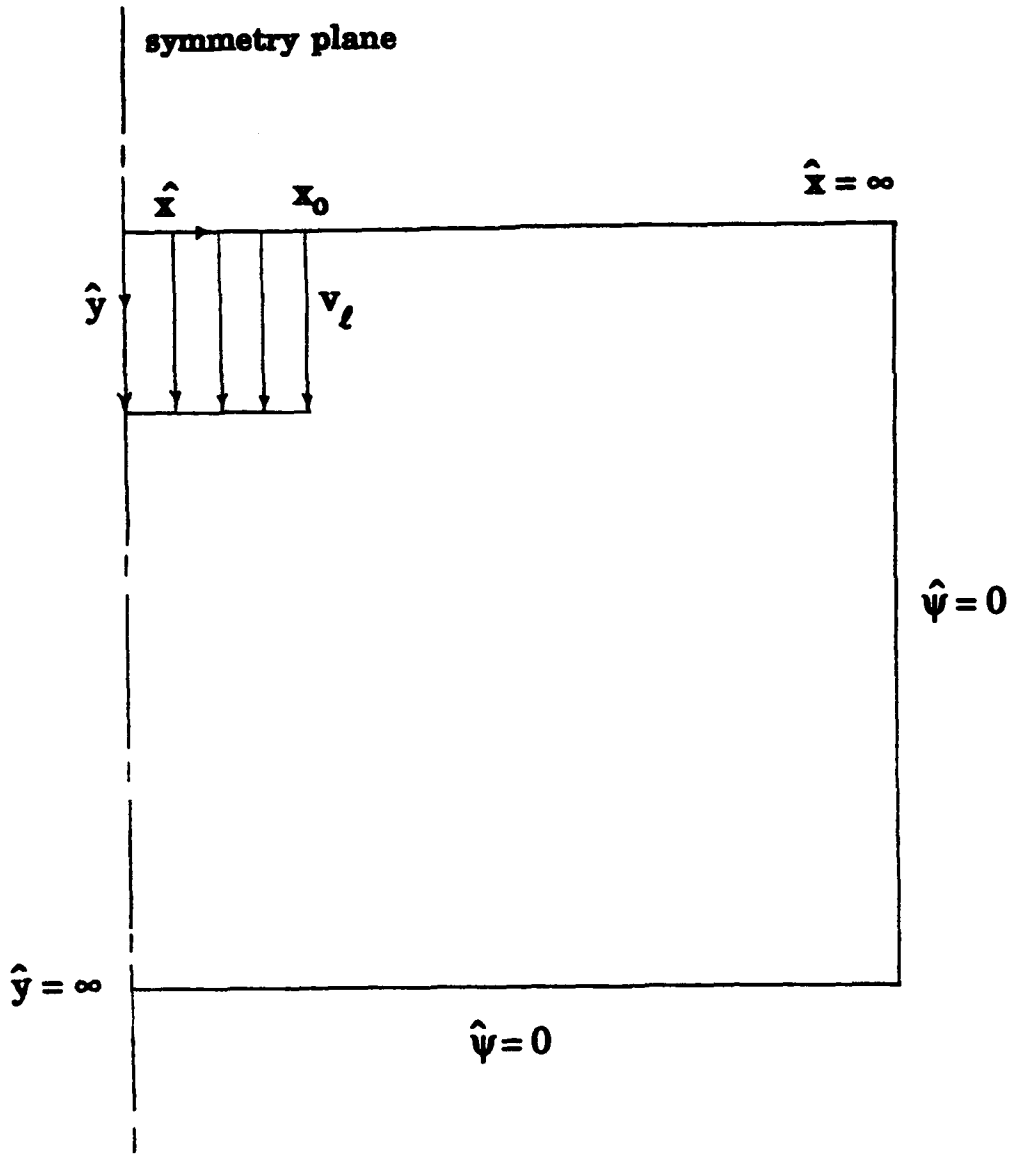

Figure 2 **Boundary conditions for the stream function**

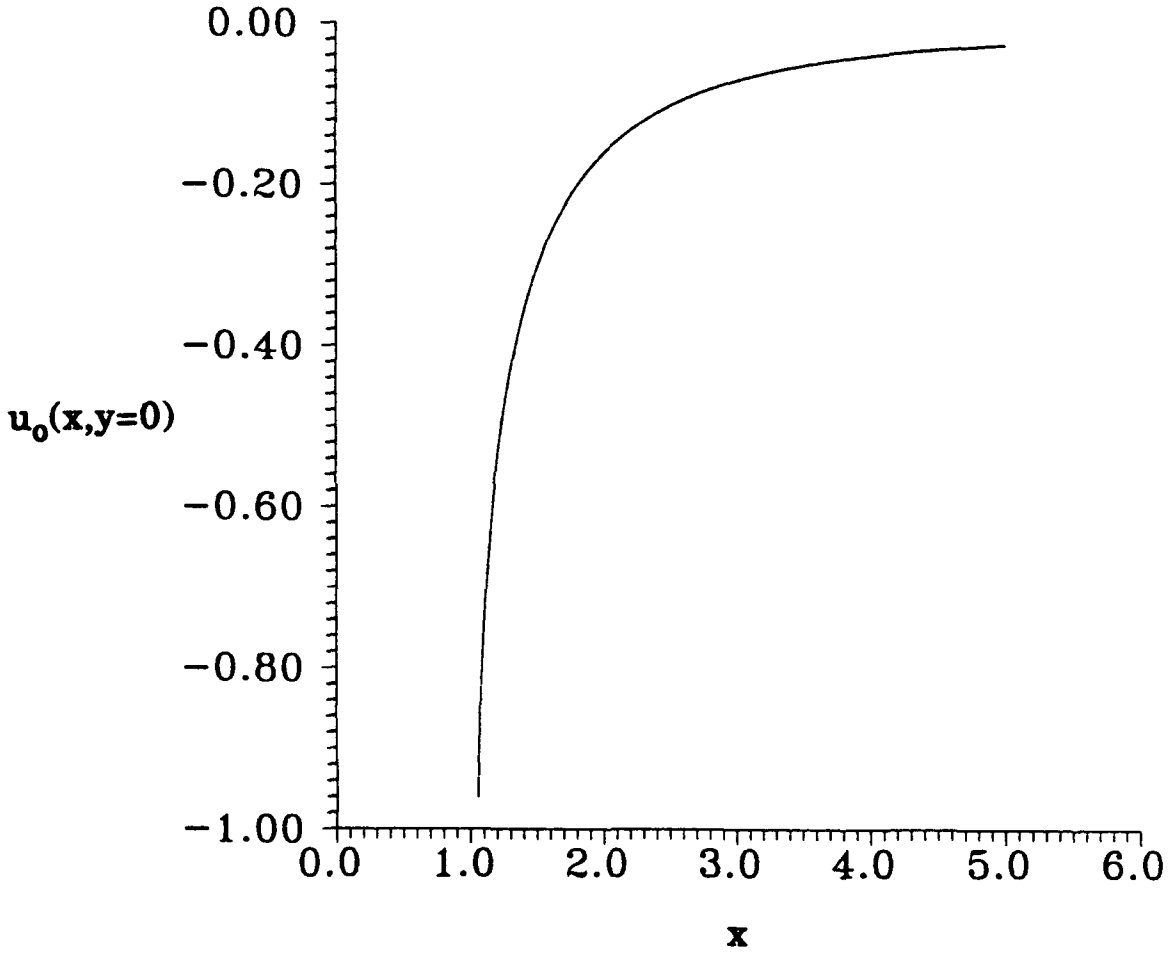

Figure 3 **Solution of the transverse velocity of order zero at the undisturbed surface level, $u_0(x,y=0)$**

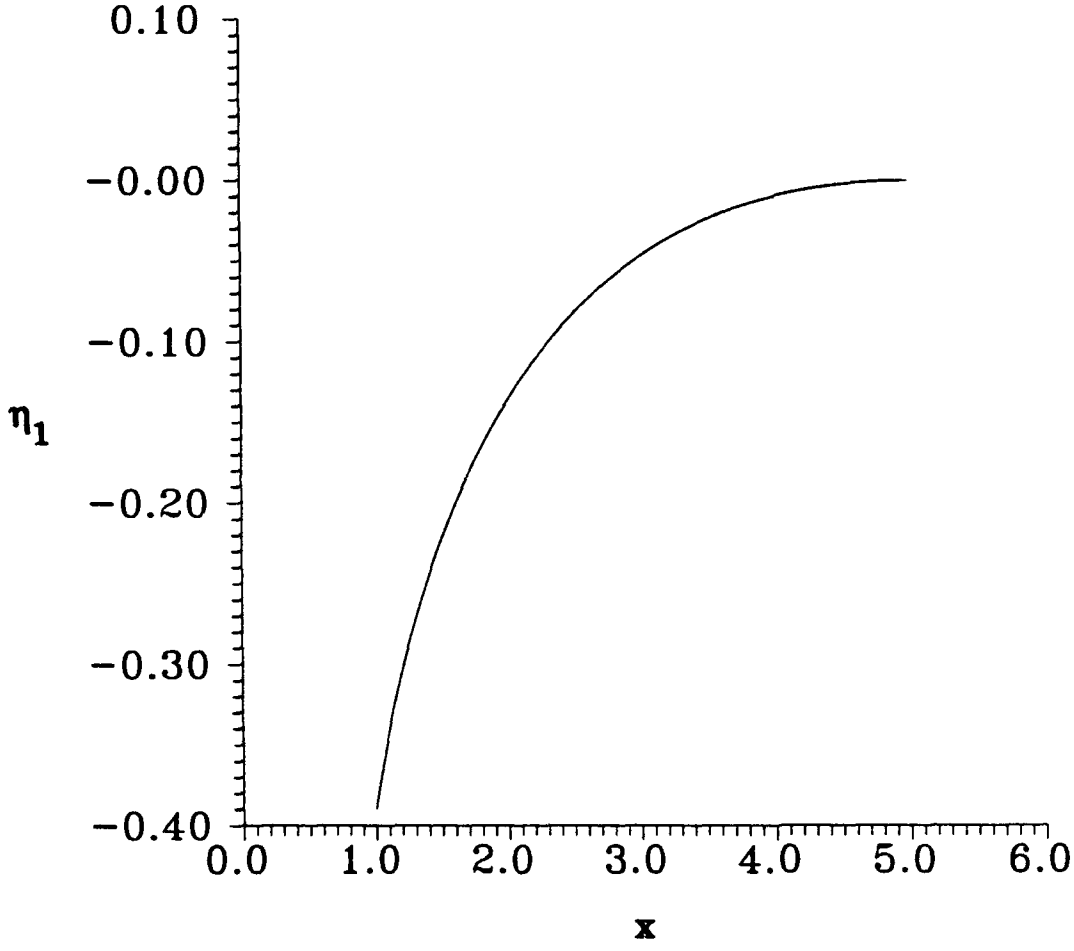

Figure 4 **First order eigenfunction of the surface position, $\eta_1(x)$**

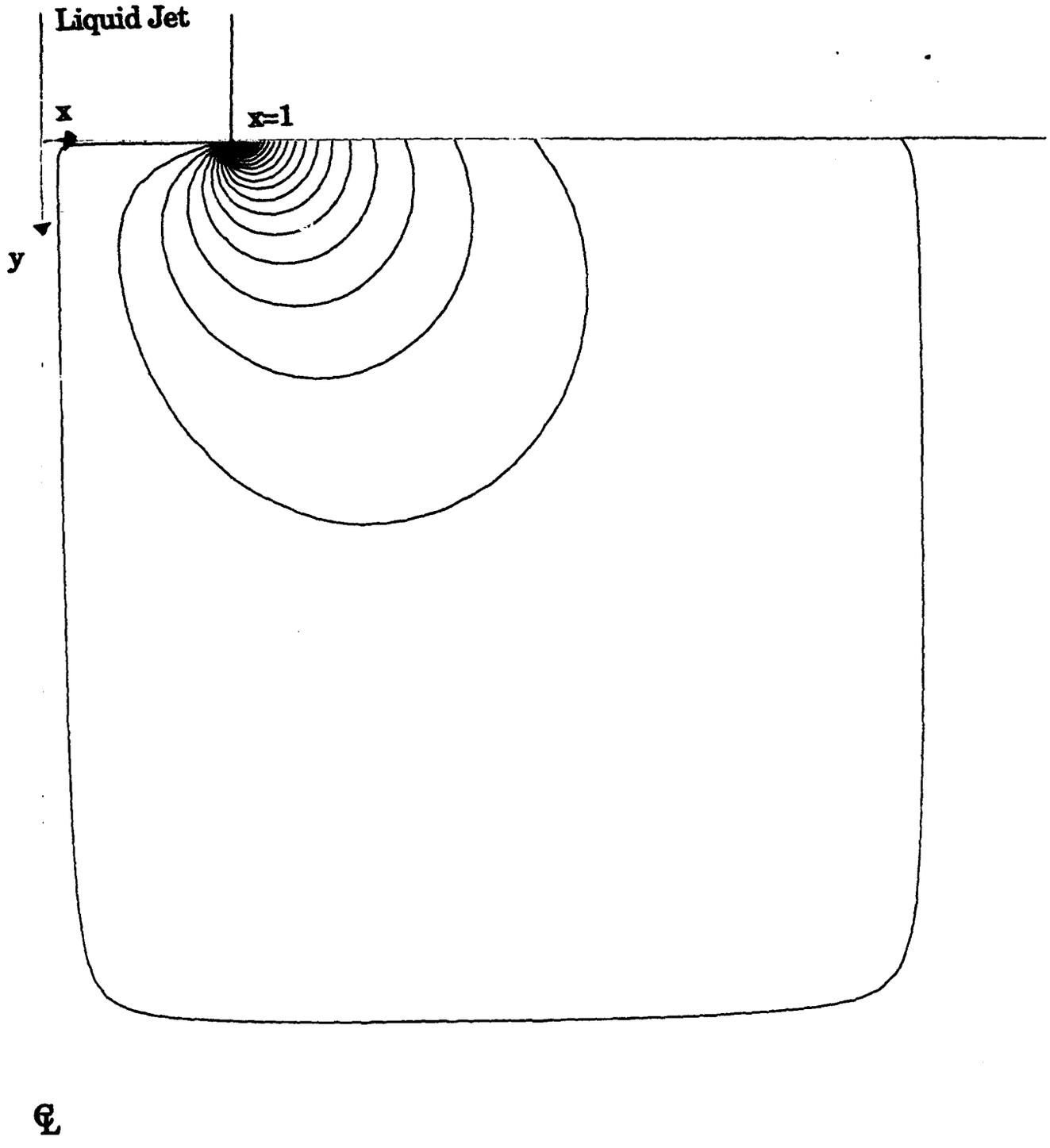

Figure 5 Contour plot of the stream function, $\psi_1(x,y)$

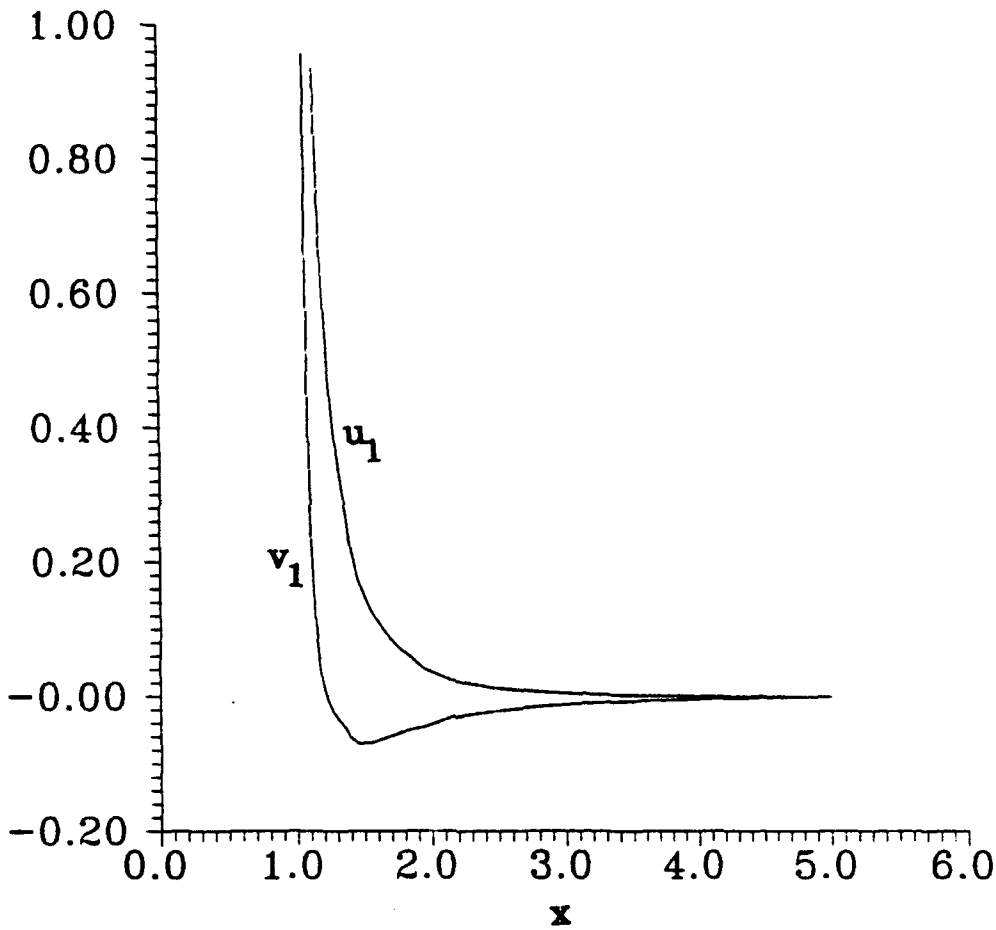

Figure 6 **Numerical solution of the transverse and axial velocities of order one, $u_1(x,y=0)$ and $v_1(x,y=0)$, respectively.**

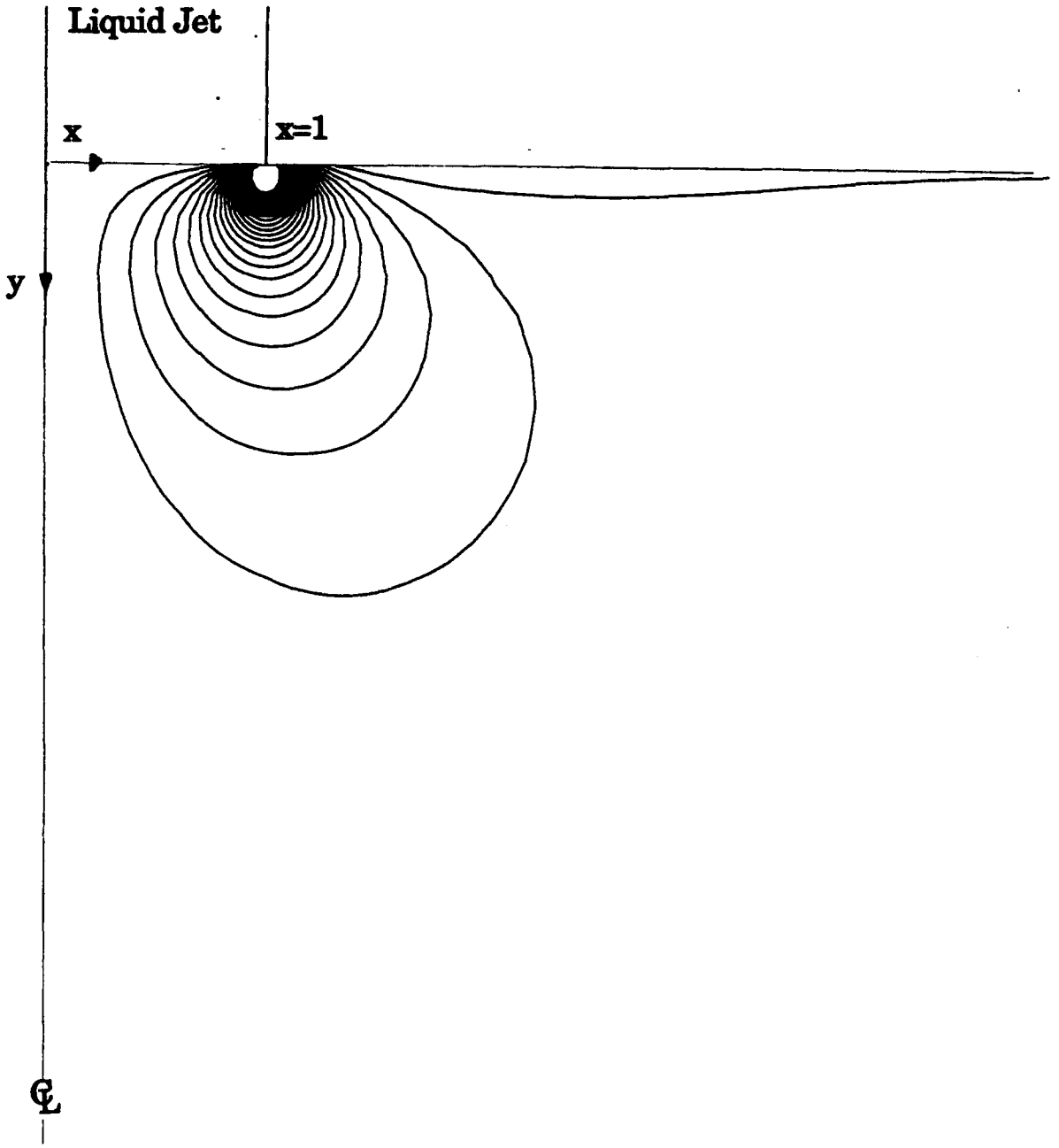

Figure 7 Contour plot of the stream function, $\psi_2(x,y)$

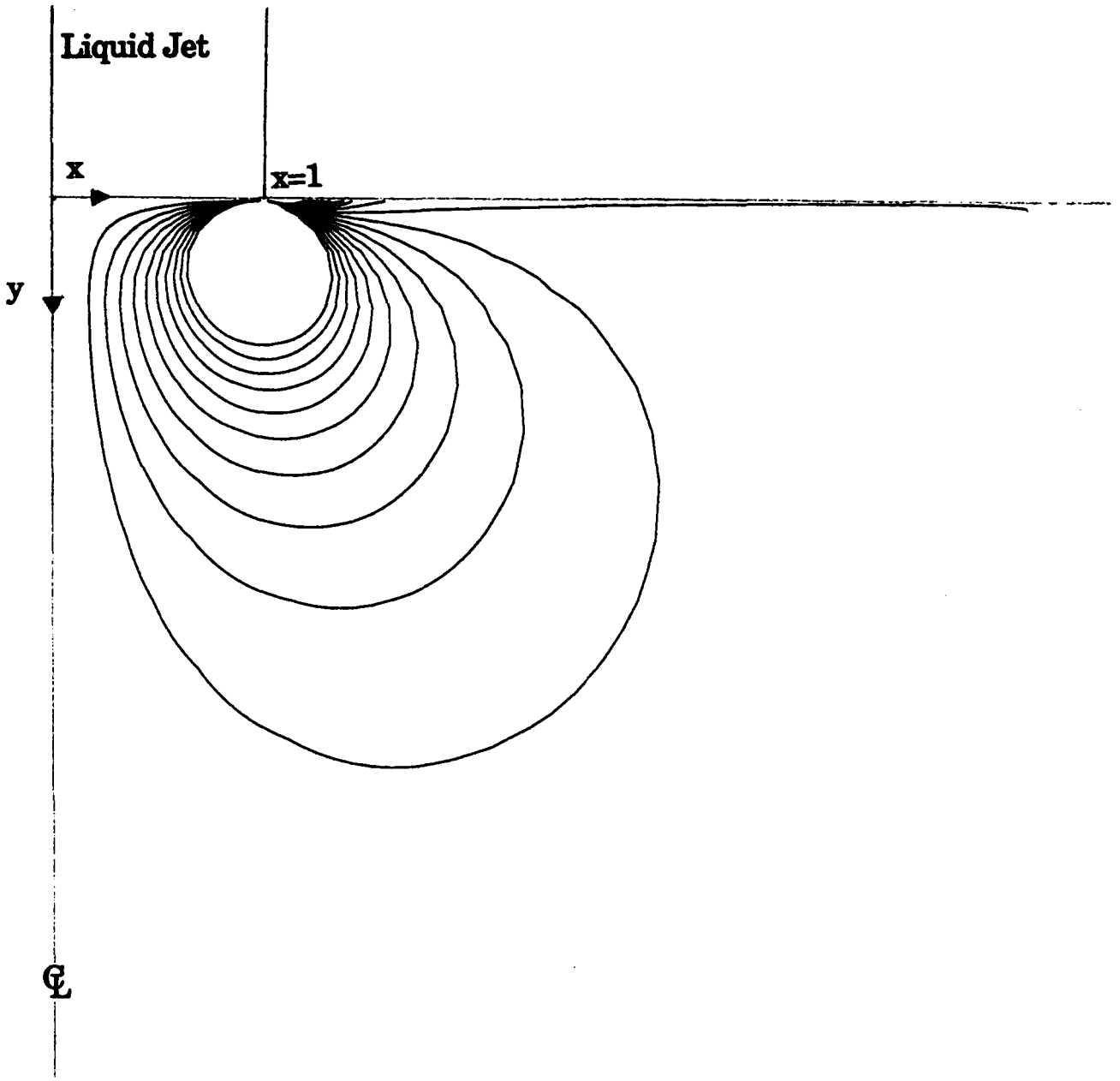

Figure 8 Contour plot of the stream function, $\psi_3(x,y)$

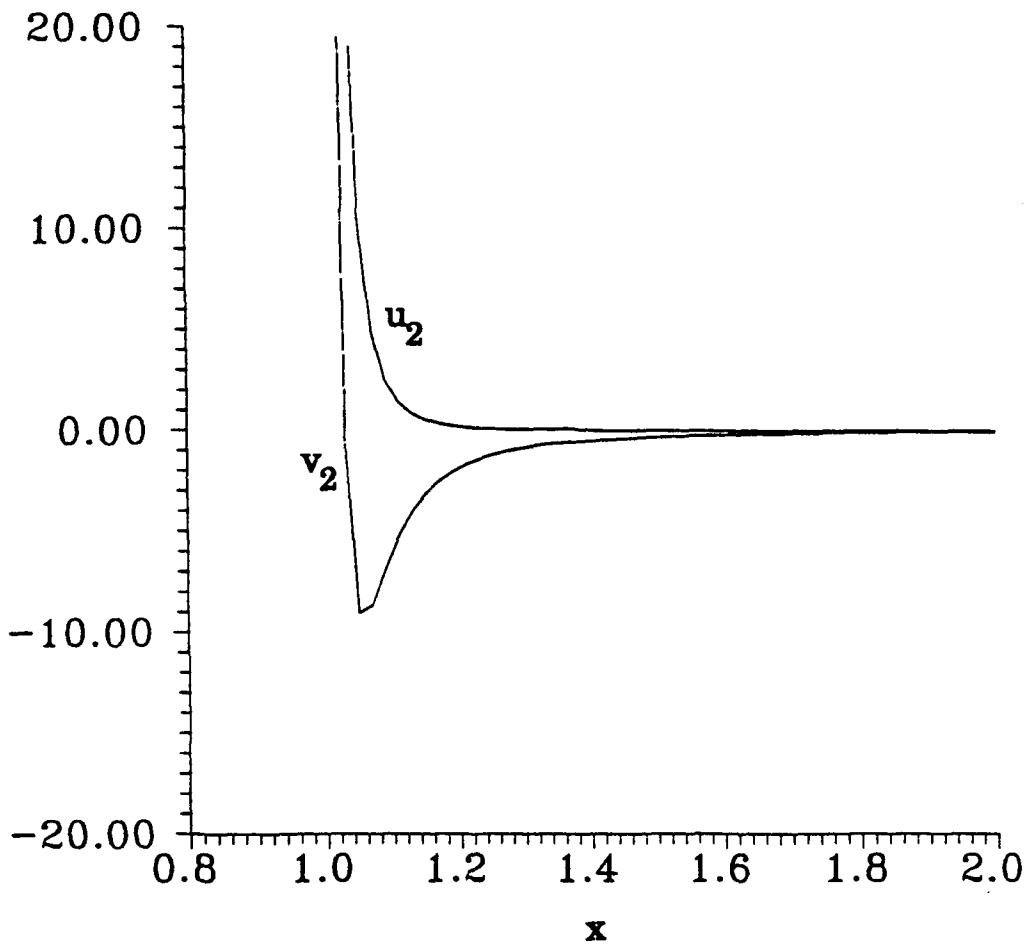

Figure 9 Numerical solution of the transverse and axial velocity of order two, $u_2(x,y=0)$ and $v_2(x,y=0)$, respectively.

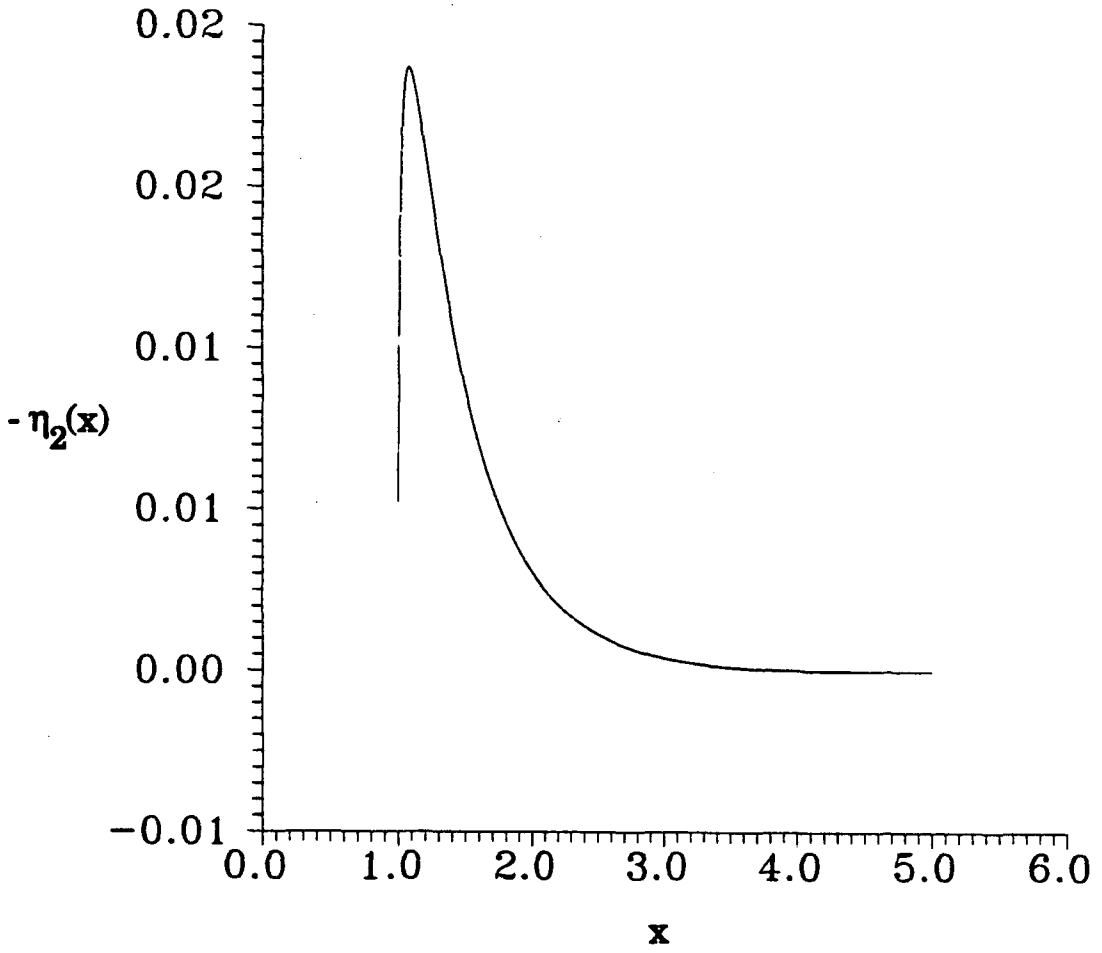

Figure 10 Second order eigenfunction of the surface position, $\eta_2(x)$

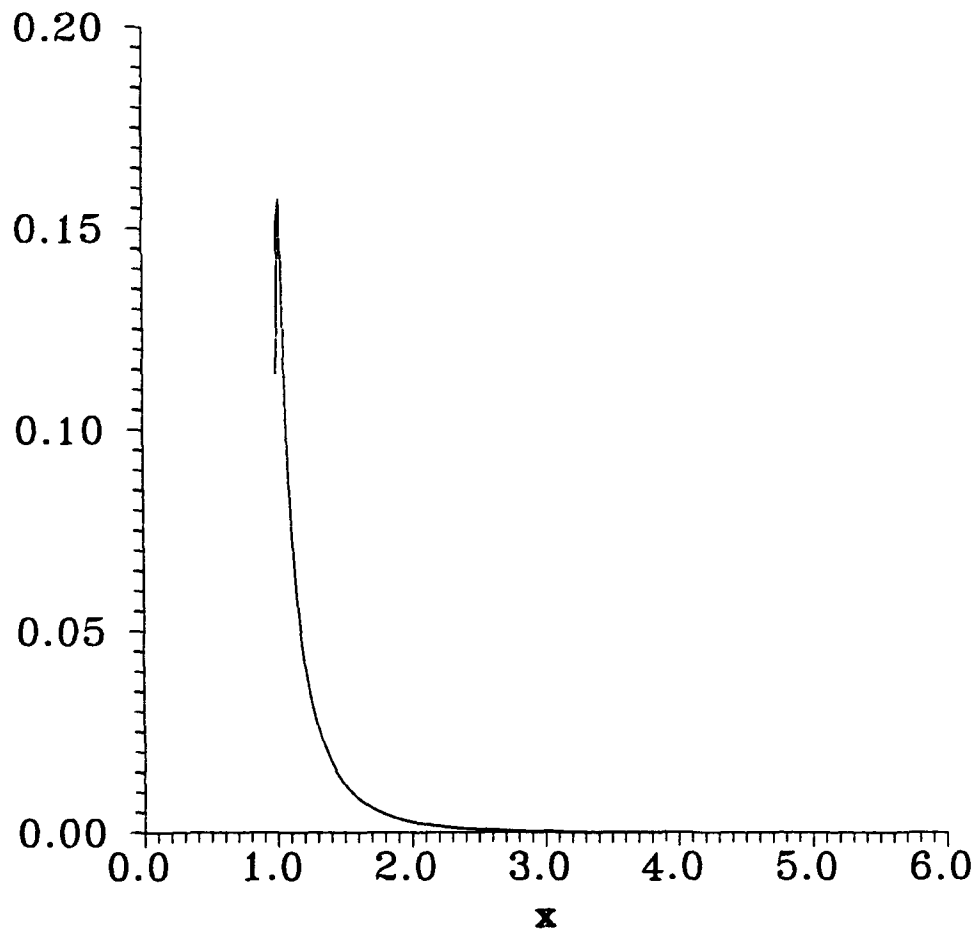

Figure 11 Third order eigenfunction of the surface position, $\eta_3(x)$

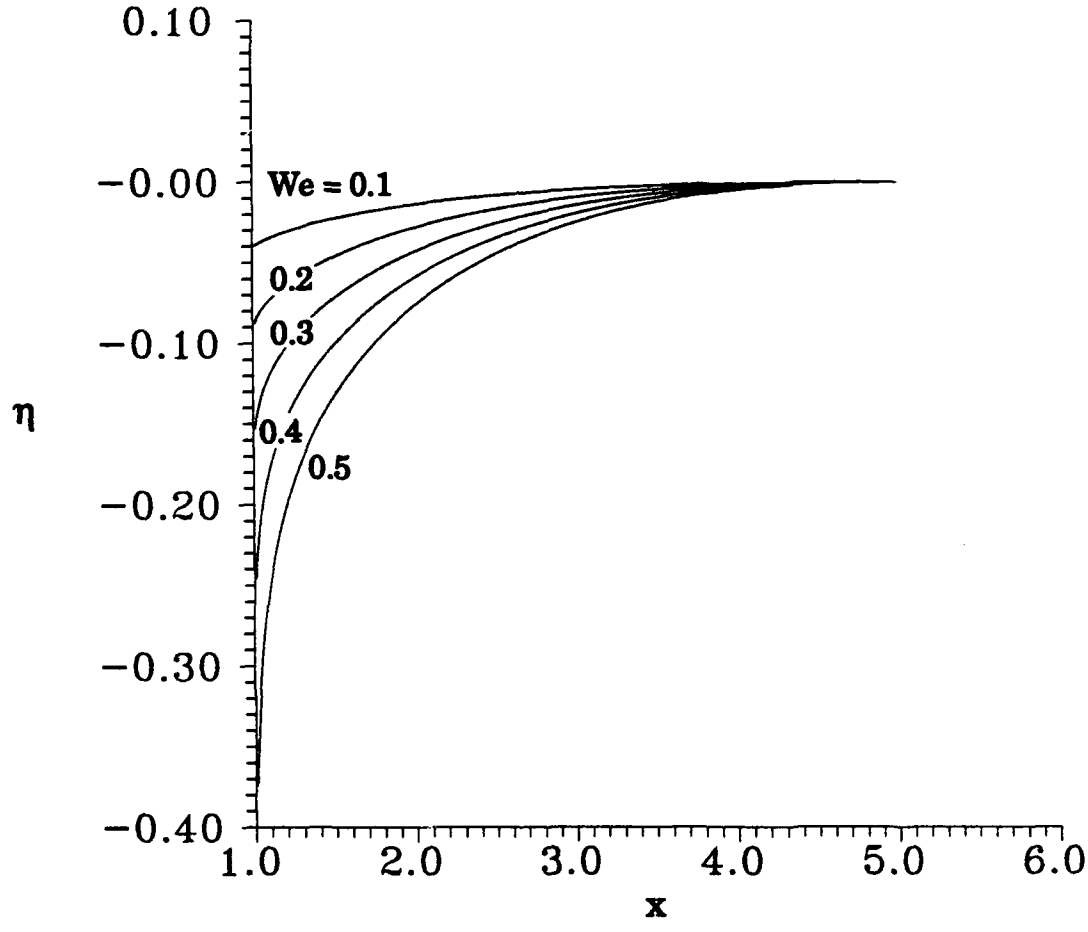

Figure 12 Shape of the interface for different Weber numbers

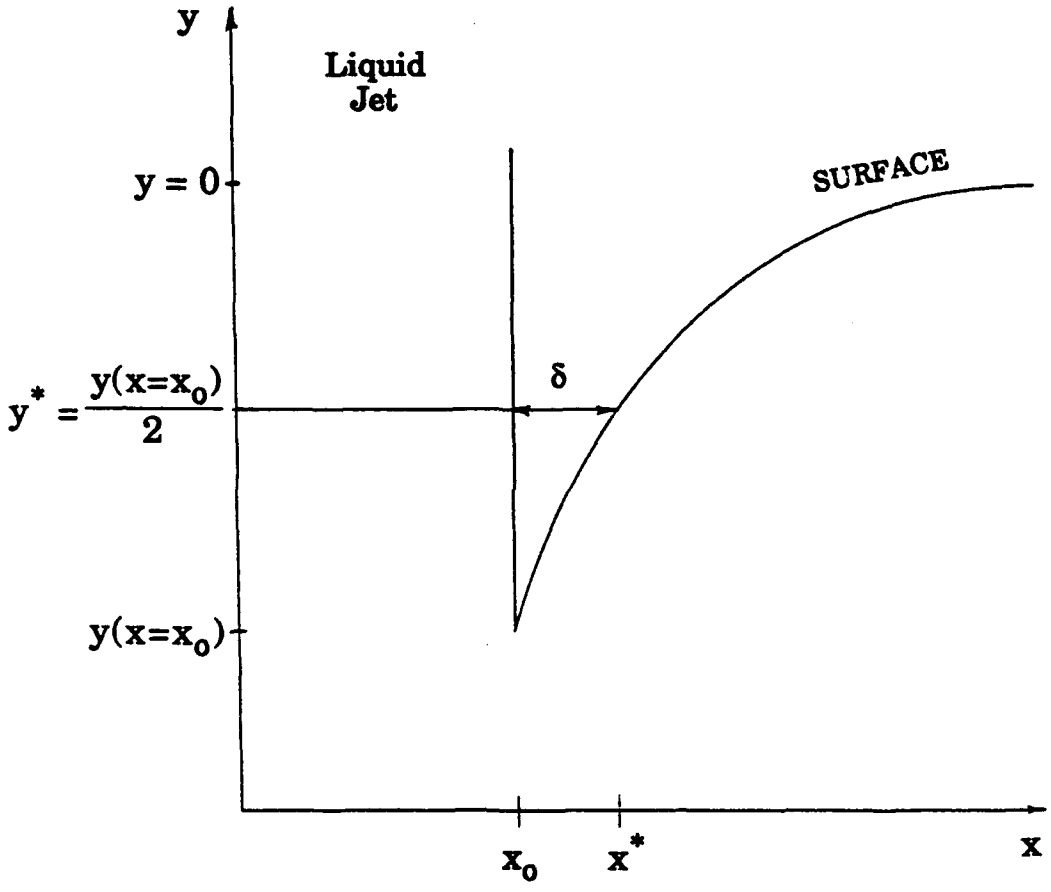

Figure 13 Definition of the gas gap width, δ

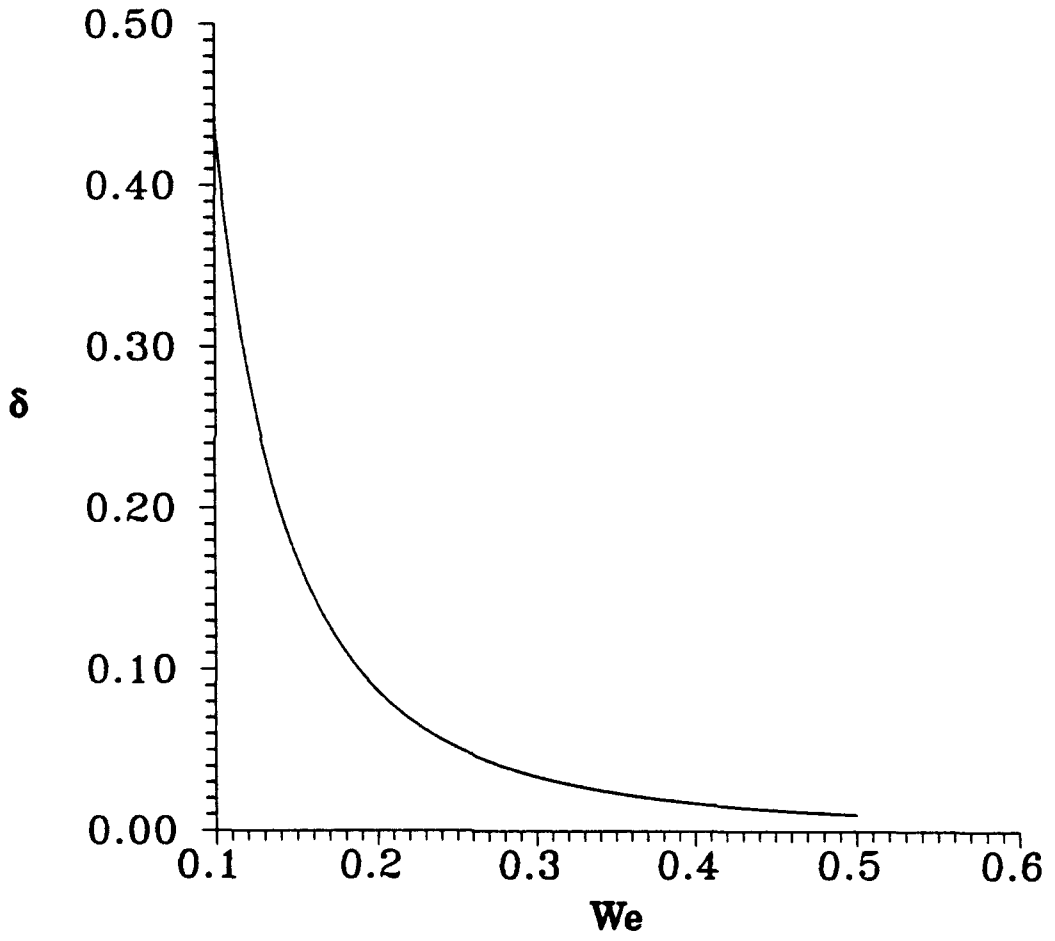

Figure 14 Gas gap width δ as a function of the We number